Author(s): Korhonen, T. & Puska, M. J. & Nieminen, Risto M.

Title: Vacancy-formation energies for fcc and bcc transition metals

Year: 1995

Version: Final published version

Please cite the original version:

Korhonen, T. & Puska, M. J. & Nieminen, Risto M. 1995. Vacancy-formation energies for fcc and bcc transition metals. Physical Review B. Volume 51, Issue 15. 9526-9532. ISSN 1550-235X (electronic). DOI: 10.1103/physrevb.51.9526.

Vacancy-formation energies for fcc and bcc transition metals

T. Korhonen, M. J. Puska, and R. M. Nieminen
Laboratory of Physics, Helsinki University of Technology, FIN-02150 Espoo, Finland
(Received 28 November 1994)

We have performed first-principles total-energy calculations for vacancy-formation energies in six bcc (V, Cr, Nb, Mo, Ta, W) and six fcc (Ni, Cu, Pd, Ag, Pt, Au) transition metals within the local-density approximation of the density-functional theory. The calculations are done using the full-potential linear-muffin-tin-orbital method employing the supercell technique. The calculated vacancy-formation energies are in good agreement with experiments especially for the fcc metals, but in the case of V and Cr the calculated values are significantly larger than the experimental ones.

I. INTRODUCTION

The knowledge of the properties of vacancies is necessary for understanding the thermodynamic and kinetic behavior of metals. The most important quantity is the vacancy-formation energy E_v^f, which determines the equilibrium vacancy concentration and contributes to the self-diffusion coefficient in the monovacancy mechanism, which is the main diffusion process in close-packed metals as well as in the bcc iron.[1] The activation energy for self-diffusion Q_v^{sd} is the sum of the vacancy-formation energy E_v^f and of the migration energy of the vacancy E_v^m. Experimentally the vacancy properties are very difficult to obtain, because very pure samples and a small concentration of thermal vacancies are required for reliable results. The theoretical approach is not easy either. While the properties of perfect crystals are obtained from standard first-principles density-functional calculations, the calculations for point defects are much more difficult because of the loss of translational symmetry. This problem is usually solved by using either supercell or Green's-function methods. For vacancies in simple metals, there have been several calculations.[1–10] However, in the case of transition metals, for which pseudopotential methods are difficult to apply, calculations of vacancy properties are much more scarce.[11–14]

For the transition metals, there exists experimental vacancy-formation energies[15,16] to compare with and thereby one can get an idea about the importance of different approximations used in the calculations. Especially interesting are the effects due to the local-density approximation (LDA) for the electron exchange and correlation energy. The vacancy-formation energy suits this purpose very well, because one need not calculate the energy of an isolated atom, which is a source of error when comparing the experimental and theoretical cohesive energies. When calculating vacancy-formation energy, there is no core electron energy problem because of the cancellation of errors, and in a metal the basic concept of an electron gas is better satisfied than is the case for an atom. Actually, in our calculations, the LDA is expected to be the most severe approximation. This is because we can control the errors due to the numerical approximations. Also, the errors due to the omission of the lattice relaxation of the atoms neighboring the vacancies are only of the order of one-tenth of an eV,[1,3,9] and thus are about one order in magnitude smaller than the typical LDA errors in binding energies.[17]

In this paper, we present results of first-principles density-functional calculations for the vacancy-formation energies of six bcc (V, Cr, Nb, Mo, Ta, W) and six fcc (Ni, Cu, Pd, Ag, Pt, Au) metals. We have omitted the lattice relaxation around the vacancy and used the supercell approach in our full-potential linear-muffin-tin-orbital (FP-LMTO) calculations.[18,19] Because the results for different metals are obtained using the same basic assumptions, reliable studies of the trends along the transition metal series are possible. The organization of the present paper is as follows. In Sec. II, we describe the computational details. Section III contains the results obtained and their discussion. Section IV is a short summary.

II. COMPUTATIONAL METHOD

The self-consistent electronic structure calculations presented here are based on the density-functional theory within the LDA.[17] In practice, we use the form suggested by Perdew and Zunger[20] to interpolate between the results by Ceperley and Alder[21] for the exchange and correlation energy in a homogeneous electron gas. The Kohn-Sham equations are solved using the FP-LMTO method.[18,19] The basis for one-particle wave functions consists of s, p, and d partial waves with kinetic energies of $-\kappa^2 = -0.01$ and -1.0 Ry centered on the ideal lattice sites; thus, 18 functions per sphere are used. The density and potential are expanded in spherical harmonics up to angular momentum $l_{max} = 4$ inside the spheres. The **k**-space integrations are performed with an evenly distributed point mesh of 16 and 10 irreducible points for the bcc and fcc supercells, respectively. For a better numerical stability, each sampled energy is broadened with a Gaussian having $\sigma = 20$ mRy.

As a matter of fact, the use of the full nonsphericity of charge density is essential in order to get accurate vacancy-formation energies.[2,11,12] The atomic-sphere ap-

proximation (ASA), which gives quite reasonable structural properties of bulk systems (e.g., the lattice constant, elastic constants), does not give reliable total energies for defects.[2,14]

In the calculations for the vacancies supercells with 27 and 32 lattice sites for bcc and fcc metals are used, respectively. For the lattice constants, the values optimized for perfect crystals are employed and the atoms neighboring the vacancies are not allowed to relax from their perfect lattice positions. The total energies of bulk metals are also calculated in the same supercell geometry in order to have better cancellation of numerical errors.

III. RESULTS AND DISCUSSION

The calculated lattice constants ($a_0^{\mathrm{FP-PW}}$) and bulk moduli ($B^{\mathrm{FP-PW}}$) are summarized in Table I together with the experimental data[22] (a_0^{exp} and B^{exp}) and results of several previous calculations. The table shows the FP-LMTO results by Körling and Häglund[23] and the LMTO-ASA results by Ozoliņš and Körling.[24] Both calculations are performed using the LDA as well as the generalized gradient approximation (GGA).[23] Also shown are the Korringa-Kohn-Rostoker (KKR) results by Moruzzi *et al.*[25] It is seen that the FP-LMTO-LDA underestimates lattice constants, especially in the beginning of the 3*d* series. The underestimation is a well-known deficit of the LDA. The FP-LMTO-GGA values seem to be in good agreement with the experimental data. The effect of the ASA is to increase the equilibrium volume of the crystal compensating thereby the contraction predicted by the LDA. The bulk modulus is seen to follow the well-known parabolic behavior in the *d* series. The slight discrepancy between our FP-LMTO-LDA calculations (FP-PW) and those of Ref. 24 (FP-LMTO-LDA) is most probably due to the fact that in Ref. 24 the basis set contains also *f* functions with the kinetic energy of $-\kappa^2 = -0.01$ Ry and that there the extended 4*p* states of the 4*d* metals were treated as semicore states.

In the supercell approximation, the vacancy-formation energy is a function of the size of the supercell and it reads[6,26]

$$E_v^f(N) = E(N-1,1,\tilde{\Omega}) - \frac{N-1}{N}E(N,0,\Omega), \qquad (1)$$

where $E(N,v,\Omega)$ is the total energy of a supercell containing N atoms and v vacancies at a volume Ω. We assume that the lattice parameter is not affected by the formation of the vacancy, i.e., $\tilde{\Omega} = \Omega = N\Omega_0$, where Ω_0 is the equilibrium volume per atom in the corresponding bulk system. In Fig. 1 the charge density of the ideal supercell, that of the vacancy supercell, and their difference are shown in the case of vanadium supercell size of $N = 27$. In Fig. 2, the corresponding charge densities for copper are shown for the supercell size of $N = 32$. The charge density differences near the nuclei seem to be quite large but they are in fact very small compared to the unperturbed density. (The figures show the total charge density.) As seen from the figures, the electronic screening in metals is very effective and we expect that the vacancies are essentially isolated in the supercells used, which should be the case because we are not relaxing the atoms from their ideal lattice sites. It has been shown that the electronic part for the formation energy converges very rapidly with respect to the supercell size, whereas the elastic part (i.e., the part connected to the relaxation of atomic positions) converges more slowly

TABLE I. Calculated and experimental lattice constants and bulk moduli for the 12 metals studied. FP-PW denotes the present FP-LMTO results within the LDA. The FP-LMTO values within the LDA (FP-LDA) and within the GGA (FP-GGA) are taken from Ref. 24. The LMTO-ASA values within the LDA (ASA-LDA) and within the GGA (ASA-GGA) are taken from Ref. 23. The KKR values are from Ref. 25 and the experimental (exp) values are from Ref. 22. The lattice constants are in atomic units (1 a.u. = 0.52175 Å) and the bulk moduli in Mbar. Δa is the difference between the calculated lattice constants ($a_0^{\mathrm{FP-PW}}$) and the experimental values (a_0^{exp}).

	V	Cr	Ni	Cu	Nb	Mo	Pd	Ag	Ta	W	Pt	Au
	bcc	bcc	fcc	fcc	bcc	bcc	fcc	fcc	bcc	bcc	fcc	fcc
$a_0^{\mathrm{FP-PW}}$	5.49	5.25	6.47	6.66	6.04	5.84	7.27	7.58	6.08	5.89	7.39	7.68
$a_0^{\mathrm{FP-LDA}}$	5.53				6.14	5.88	7.25		6.07	5.88	7.36	
$a_0^{\mathrm{FP-GGA}}$	5.66				6.25	5.97	7.45		6.21	5.98	7.51	
$a_0^{\mathrm{ASA-LDA}}$	5.63	5.37	6.54		6.28	6.02	7.37		6.28	6.07	7.51	
$a_0^{\mathrm{ASA-GGA}}$	5.71	5.45	6.70		6.39	6.11	7.53		6.38	6.15	7.65	
a_0^{KKR}	5.54	5.30	6.55	6.76	6.20	5.89	7.42	7.79				
a_0^{exp}	5.73	5.44	6.65	6.82	6.24	5.95	7.35	7.73	6.24	5.97	7.41	7.71
Δa (%)	-4.2	-3.5	-2.7	-2.6	-3.2	-1.8	-1.1	-1.9	-2.6	-1.3	-0.3	-0.4
$B^{\mathrm{FP-PW}}$	1.85	2.93	2.65	1.92	1.56	2.64	2.32	1.42	1.94	3.29	3.05	1.93
$B^{\mathrm{FP-LDA}}$	2.12				1.89	2.97	2.26		1.87	3.05	3.06	
$B^{\mathrm{FP-GGA}}$	1.08				1.67	2.59	1.71		1.75	2.71	2.63	
$B^{\mathrm{ASA-LDA}}$	1.99	2.87	2.68		1.76	2.63	2.18		2.05	3.03	2.91	
$B^{\mathrm{ASA-GGA}}$	1.84	2.20	2.53		1.66	2.42	2.09		1.83	2.72	2.32	
B^{KKR}	1.64	2.70	2.20	1.55	1.68	2.51	1.70	1.02				
B^{exp}	1.62	1.90	1.86	1.37	1.70	2.73	1.81	1.01	2.00	3.23	2.78	1.73

with the increasing supercell size.[1,3,4]

In Table II, the dependence of the vacancy-formation energy on the supercell size (N) and on the number of $\mathbf{k}$ points (nk) is summarized in the case of vanadium. It is seen that the convergence with respect to the $\mathbf{k}$-space summations is achieved for the supercell sizes of $N = 8$ and $N = 16$. It is also reasonable to suppose that $nk = 16$ is sufficient for $N = 27$. The convergence with the increasing supercell size is less satisfactory. There seems to be non-negligible attractive interactions between vacancies in the $N = 8$ and $N = 16$ supercells, where the vacancy-vacancy distances are 1.73 and 2.0 lattice constants, respectively, and there is only one atom between the nearest vacancies. In the case $N = 27$, the distance between vacancies is 2.6 lattice constants and there are two atoms between the nearest vacancies, so that the interactions between vacancies are weaker. This is also seen from Fig. 1. In the $N = 27$ case,

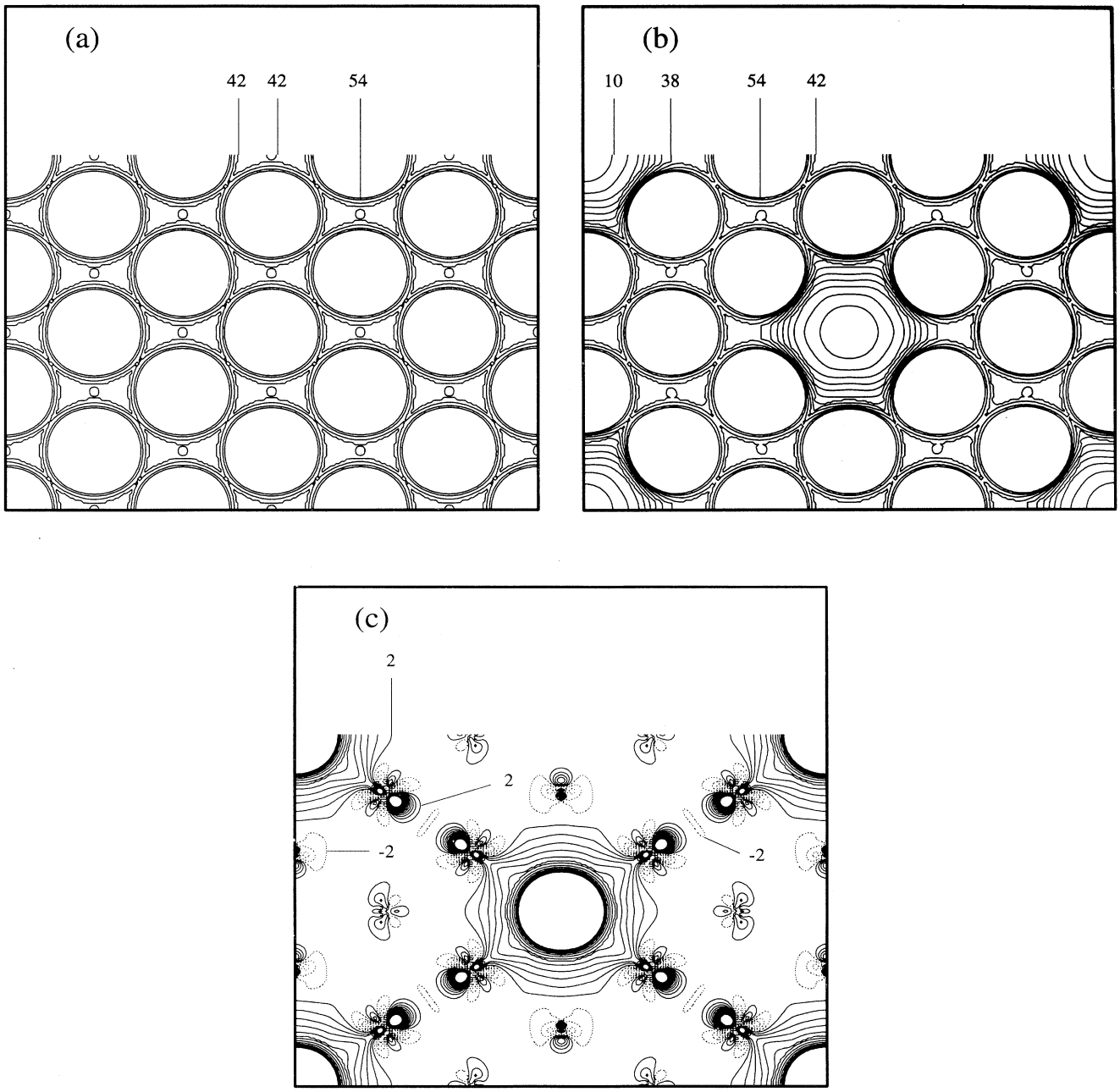

FIG. 1. Electron density in vanadium (a) for a perfect supercell, (b) for a vacancy supercell, and (c) the difference between (a) and (b). In (c) the solid line is for positive difference and dashed line for negative one. The size of the supercell is $N = 27$ and the plane of the figures is the (110) plane. Units are in 0.001 bohr^{-3} and the spacing between contour lines is 4 units.

the induced charge difference between the two atoms on the line connecting the vacancies is vanishingly small, whereas in the case of $N = 16$, there is a coupling between the vacancies mediated by the atoms in the $\langle 001 \rangle$ direction. In conclusion, we believe that the vacancy-formation energy obtained with $N = 27$ has converged with an accuracy much better than the difference between the $N = 16$ and $N = 27$ results, i.e., 0.3 eV. For the fcc lattice the effect of the supercell size and the number of the **k** points were not studied because of limited computational resources. It is seen from Fig. 2 that the charge density of the vacancy supercell relaxes very rapidly to the bulk value. The vacancy induced perturbation is localized within the first nearest-neighbor shell around the vacancy. The comparison with Fig. 1 and the convergence test made for bcc vanadium assures us that $N = 32$ and $nk = 10$ are enough to obtain the formation energies for the fcc structures with a reasonable

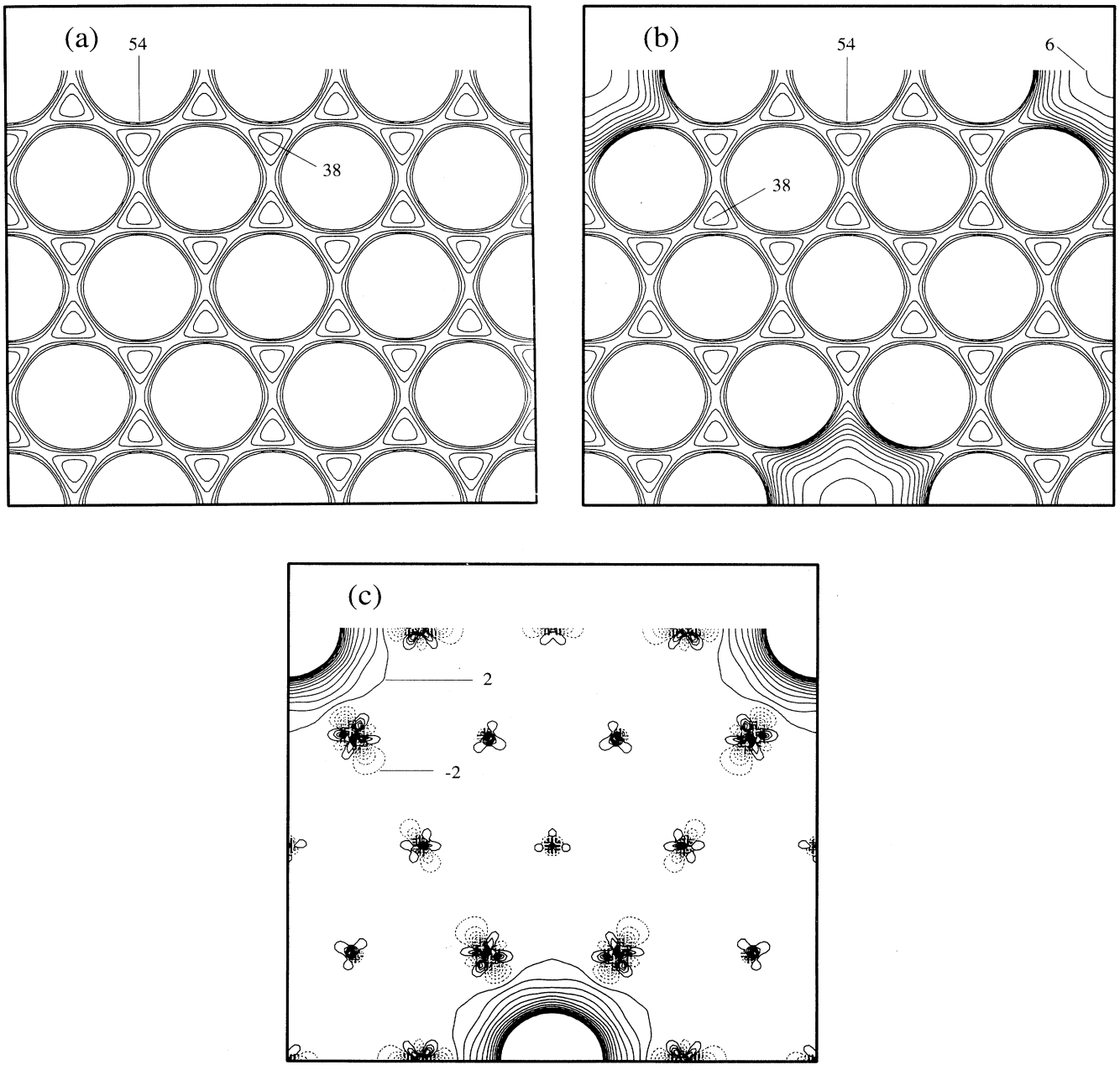

FIG. 2. Electron density in copper (a) for a perfect supercell, (b) for a vacancy supercell, and (c) difference between (a) and (b). In (c) the solid line is for positive difference and dashed line for negative one. The size of the supercell is $N = 32$ and the plane of the figures is the (111) plane. Units are in 0.001 bohr^{-3} and the spacing between contour lines is 4 units.

TABLE II. Vacancy-formation energy of vanadium as a function of the supercell size (N) and the number of the **k** points (nk) in the irreducible Brillioun zone.

$N = 8$		$N = 16$		$N = 27$	
nk	E_v^f (eV)	nk	E_v^f (eV)	nk	E_v^f (eV)
29	2.75	10	2.70	8	2.98
47	2.78	20	2.77	16	3.06
72	2.78	35	2.77		

precision with respect to the experimental uncertainties and the effects of the neglected relaxation energy of the lattice.

The calculated values for the vacancy-formation energies are given in Table III together with the previous theoretical estimates and experimental data. In Fig. 3, the present theoretical cohesion and vacancy-formation energies are compared with the experimental ones and trends are studied along the different columns of the Periodic Table. The theoretical cohesive energies are systematically of the order of 1–2 eV larger than the experimental ones. This reflects the LDA overbinding and also the effect of the approximation of the spherical charge density,[27] made in the calculation of free atom energies. In the case of the early bcc metals of the d series the experimental vacancy-formation energy obeys as a function of the atomic number a similar increasing trend as the cohesion energy. The theoretical vacancy-formation energies for the bcc metal columns show much weaker dependencies. These different trends are due to the large discrepancies in the case of V and Cr. For Nb, Ta, Mo, and W the theoretical values are closer to the experimental ones. The theoretical and experimental vacancy-formation energies for the late fcc metal columns show slightly decreasing dependencies as a function of the atomic number, whereas the cohesive energies show a minimum at the $4d$ elements. Also the absolute values of the formation energies are in a much better agreement than in the case of the bcc metals studied. Also the now omitted lattice relaxation energies should be smaller for the more densely packed fcc lattices than for the more open bcc lattices.

When studied along the rows of the Periodic Table (see Table III), the calculated vacancy-formation energies increase at the beginning and decrease at the end of the different d series. This means that the vacancy-formation energies follow the general trend known from the cohesion[25] and surface[28] energies. The parabolic trend in the cohesion properties arises from the fact that when going from left to right on transition metal series the number of d electrons increases. When adding electrons in the d states one first occupies the bonding states and after the band is half full one starts to occupy the antibonding states; one obtains the parabolic shape for the strength of d bonds.

The trends observed in the cohesive properties are of-

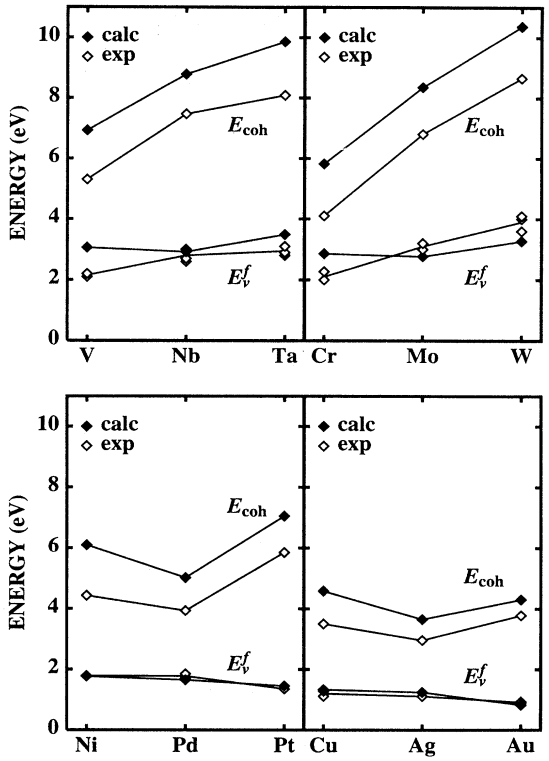

FIG. 3. Theoretical (filled symbols) and experimental (Ref. 22) (unfilled symbols) cohesion energies E_{coh} and vacancy-formation energies E_v^f of the 12 transition metals studied.

TABLE III. Theoretical and experimental values for the vacancy-formation energies. A supercell size of $N = 27$ has been used for bcc metals and a size of $N = 32$ for fcc metals. Also the results of the other known full-potential calculations are shown.

E_v^f (eV)	V bcc	Cr bcc	Ni fcc	Cu fcc	Nb bcc	Mo bcc	Pd fcc	Ag fcc	Ta bcc	W bcc	Pt fcc	Au fcc
FP-LMTO	3.06	2.86	1.77	1.33	2.92	3.13	1.65	1.24	3.49	3.27	1.45	0.82
Experiment	2.2[a]	2.27[a]	1.79[a]	1.28[a]	2.6[b]	3.0[a]	1.70[a]	1.11[a]	2.8[b]	3.6–4.1[a]	1.35[a]	0.93[a]
	2.1[b]	2.0[b]	1.78[b]	1.28[b]	2.7–3.0[a]	3.2[b]	1.85[b]	1.11[b]	2.9[b]	4.0[b]	1.32[b]	0.89[b]
				1.19[c]					3.1[a]	4.1[b]		
Other calc.			1.76[d]	1.41[d]			1.57[d]	1.20[d]				
				1.29[e]				1.06[e]				

[a]Reference 15.
[b]Reference 16.
[c]Reference 30.
[d]Reference 13.
[e]Reference 12.

TABLE IV. The values of the ratio $E_v^f/E'_{\rm coh}$ calculated from the theoretical vacancy formation and cohesive energies.

Metal	$E_v^f/E'_{\rm coh}$	Metal	$E_v^f/E'_{\rm coh}$	Metal	$E_v^f/E'_{\rm coh}$	Metal	$E_v^f/E'_{\rm coh}$
V	0.32	Cr	0.27	Ni	0.27	Cu	0.28
Nb	0.27	Mo	0.26	Pd	0.33	Ag	0.33
Ta	0.32	W	0.26	Pt	0.20	Au	0.19

ten explained in a simple bond cutting model. In this model, the energy per atom depends linearly on its local coordination number (i.e., it is a constant times the number of the nearest-neighbor bonds). This model works well for covalent materials, where the coordination is quite low and there are strong directional bonds. In metals, where the coordination is larger and bonding is more isotropic, the bond strength is approximately proportional to the square root of the coordination number.[28,29] In the second-moment approximation of the tight-binding model, the energy per atom is a function of the local coordination number of the atom,

$$E(C) = E_0 - A\sqrt{C} + BC, \tag{2}$$

where the attractive square root term takes into account the bond strength saturation and the last term is a weak repulsive term.[13,28] The parameters E_0, A, and B can be obtained from least-squares fits of calculated total energies of systems having different local coordinations.[28,29] In the case of the fcc lattice Eq. (2) is easy to apply, but for the bcc lattice one encounters the problem of how to treat the next-nearest-neighbor distances, which are only slightly longer than the nearest-neighbor distances.

We have applied the tight-binding model (2) in analyzing the vacancy-formation energies. Following Ref. 28, the parameters are determined as follows: the (small) constant term E_0 is neglected, because we are interested in energy differences only. The energy per atom in the bulk $E(C_B)$ is set equal to $-E'_{\rm coh}$, which is the negative of the cohesive energy calculated relative to the free non-spin-polarized atom. The value for B is chosen to be $B = 0.03E'_{\rm coh}$, which has been shown to give reasonable results in the case of the surface energies of the $4d$ transition metals.[28] With these choices the model gives for the ratio $E_v^f/E'_{\rm coh}$ a constant value, which depends only on the coordination number of the lattice. For the fcc this ratio is 0.33. If one neglects the repulsive term a larger constant of 0.51 is obtained. For the bcc metals one cannot get an estimate for the constant ratio because of the next-nearest-neighbor bonds. The values of the ratio $E_v^f/E'_{\rm coh}$ calculated from the theoretical vacancy formation and cohesive energies are given in Table IV. The ratios for the $3d$ and $4d$ fcc metals Ni, Pd, Cu, and Ag are quite close to the tight-binding model value of 0.33, whereas for Pt and Au the ratios are considerably lower. In the case of the bcc metals, the $E_v^f/E'_{\rm coh}$ ratios are around 0.3. As a conclusion from Table IV, one can say that the simple tight-binding model can roughly reproduce the magnitude of the ratio $E_v^f/E'_{\rm coh}$, but there exist also clear trends not explainable with this simple model.

Previous calculations exist for vacancy-formation energies for some fcc transition metals. The agreement with the present results is excellent as can be seen from Table III. Also the agreement between the present values and the experimental ones is good for the fcc metals. For the fcc metals now studied the experimental values are known quite well, except in the case of Pd for which the low purity of the samples is a problem.[15] The experimental values of the early $4d$ and $5d$ transition metals are also quite well reproduced but discrepancies are seen to occur expecially for the early $3d$ transition metals V and Cr. In the case of bcc metals, the experimental values are much more uncertain than those for the fcc metals partly due to relatively impure samples and partly due to small E_v^f/E_v^m ratios.[15] For the fcc metals, the experimental values for single vacancy diffusion data are well converged, i.e., $Q_v^{\rm sd} = E_v^f + E_v^m$, whereas for the bcc metals the situation is much worse. For the bcc metals the present calculated vacancy-formation energies are useful when comparing the different experimental values. In the future, it should be also interesting to calculate the migration energy of monovacancy diffusion for the bcc metals in order to get an estimate for the activation energy for self-diffusion in the monovacancy mechanism.

IV. CONCLUSIONS

In conclusion, it has been shown that *ab initio* full-potential calculations provide reliable values for the vacancy-formation energies of transition metals. For the fcc metals the calculated vacancy-formation energies are in good agreement with known experimental data. For the bcc metals the agreement is less satisfactory. This is partly due to the larger scatter in the experimental values, but in the case of V and Cr the calculated values are significantly, i.e., about 1 eV, larger than the experimental values. The discrepancies for V and Cr are not unexpected because the LDA is known to overbind these metals more than the metals later in the $3d$ series.[23,24] Thus these materials provide a useful testing ground for different corrections to the LDA, such as the GGA method. For some fcc metals there exists other full-potential calculations[11,13] which are in good agreement with present ones.

ACKNOWLEDGMENTS

The authors gratefully acknowledge Dr. M. Methfessel for supplying the FP-LMTO code. One of the authors (T.K.) acknowledges partial financial support by the Emil Aaltonen Foundation. This work has been made possible by generous computer resources from the Computing Center of Helsinki University of Technology and the Center of Scientific Computing, Espoo, Finland.

[1] W. Frank, U. Breier, C. Elsässer, and M. Fähnle, Phys. Rev. B **48**, 7676 (1993).
[2] T. Beuerle, R. Pawellek, C. Elsässer, and M. Fähnle, J. Phys. Condens. Matter **3**, 1957 (1991).
[3] M. J. Mehl and B. M. Klein, Physica B **172**, 211 (1991).
[4] Robert W. Jansen and Barry M. Klein, J. Phys. Condens. Matter **1**, 8359 (1989).
[5] A. De Vita and M. J. Gillan, J. Phys. Condens. Matter **3**, 6225 (1991).
[6] M. J. Gillan, J. Phys. Condens. Matter **1**, 689 (1989).
[7] B. Chakraborty, R. W. Siegel, and W. E. Pickett, Phys. Rev. B **24**, 5445 (1981).
[8] R. Benedek, L. H. Yang, C. Woodward, and B. I. Min, Phys. Rev. B **45**, 2607 (1992).
[9] R. Pawellek, M. Fähnle, C. Elsässer, K.-M. Ho, and C.-T. Chan, J. Phys. Condens. Matter **3**, 2451 (1991).
[10] P. J. H. Denteneer and J. M. Soler, J. Phys. Condens. Matter **3**, 8777 (1991).
[11] P. H. Dederichs, T. Hoshino, B. Drittler, K. Abraham, and R. Zeller, Physica B **172**, 203 (1991).
[12] B. Drittler, M. Weinert, R. Zeller, and P. H. Dederichs, Solid State Commun. **79**, 31 (1991).
[13] H. M. Polatoglou, M. Methfessel, and M. Scheffler, Phys. Rev. B **48**, 1877 (1993).
[14] P. Braun, M. Fähnle, M. van Schilfgaarde, and O. Jepsen, Phys. Rev. B **44**, 845 (1991).
[15] H. Schultz and P. Ehrhart, in *Atomic Defects in Metals*, edited by H. Ullmaier, Landolt-Börnstein, New Series, Group III (Springer, Berlin, 1991).
[16] Positron annihilation results quoted in H.-E. Schaefer, Phys. Status Solidi A **102**, 47 (1987).
[17] For a recent review, see R. O. Jones and O. Gunnarsson, Rev. Mod. Phys. **61**, 689 (1989).
[18] M. Methfessel, Phys. Rev. B **38**, 1537 (1988).
[19] M. Methfessel, C. O. Rodriguez, and O. K. Andersen, Phys. Rev. B **40**, 2009 (1989).
[20] J. Perdew and A. Zunger, Phys. Rev. B **23**, 5048 (1981).
[21] D. M. Ceperley and B. J. Alder, Phys. Rev. Lett. **45**, 566 (1980).
[22] C. Kittel, *Introduction to Solid State Physics*, 4th ed. (Wiley, New York, 1971).
[23] M. Körling and J. Häglund, Phys. Rev. B **45**, 13 293 (1992).
[24] V. Ozoliņš and M. Körling, Phys. Rev. B **48**, 18 304 (1993).
[25] V. L. Moruzzi, J. F. Janak, and A. R. Williams, *Calculated Electronic Properties of Metals* (Pergamon, New York, 1978).
[26] M. Sinder, D. Fuks, and J. Pelleg, Phys. Rev. B **50**, 2775 (1994).
[27] F. W. Kutzler and G. S. Painter, Phys. Rev. Lett. **59**, 1285 (1987).
[28] M. Methfessel, D. Hennig, and M. Scheffler, Phys. Rev. B **46**, 4816 (1992).
[29] I. J. Robertson, M. C. Payne, and V. Heine, Europhys. Lett. **15**, 301 (1991).
[30] Th. Hehenkamp, W. Berger, J.-E. Kluin, Ch. Lüdecke, and J. Wolff, Phys. Rev. B **45**, 1998 (1992).